# Supermodular interference suppression game for multistatic MIMO radar networks and multiple jammers with multiple targets[*][#]

Bin HE[1,2], Hongtao SU[‡1]

*[1]National Laboratory of Radar Signal Processing, Xidian University, Xi'an 710071, China*
*[2]The 54th Research Institute of CETC, Shijiazhuang 050081, China*
E-mail: aihebin19@163.com; suht@xidian.edu.cn

**Abstract:** To deal with the threat of the new generation of electronic warfare, we establish a non-cooperative countermeasure game model to analyze power allocation and interference suppression between multistatic multiple-input multiple-output (MIMO) radars and multiple jammers in this study. First, according to the power allocation strategy, a supermodular power allocation game framework with a fixed weight (FW) vector is constructed. At the same time, a constrained optimization model for maximizing the radar utility function is established. Based on the utility function, the best power allocation strategies for the radars and jammers are obtained. The existence and uniqueness of the Nash equilibrium (NE) of the supermodular game are proved. A supermodular game algorithm with FW is proposed which converges to the NE. In addition, we use adaptive beamforming methods to suppress cross-channel interference that occurs as direct wave interferences between the radars and jammers. A supermodular game algorithm for joint power allocation and beamforming is also proposed. The algorithm can ensure the best power allocation, and also improves the interference suppression ability of the MIMO radar. Finally, the effectiveness and convergence of two algorithms are verified by numerical results.

## 1 Introduction

With the continuous development of modern electronic warfare (EW), all countries are updating and improving their own weapons and equipment (Stephens, 1996). As the main participants in EW, new radar systems, including multiple-input multiple-output (MIMO) radar, cognitive radar, multistatic radar, and imaging radar, have become the main research and development direction of various countries. In particular, MIMO radar will be gradually applied to modern military conflicts. Multistatic MIMO radar combines the advantages of MIMO and multistatic radars, and it will become the main research direction of the next-generation radar system. It not only has superior target detection and tracking ability, but also exhibits wide coverage and strong interference suppression abilities (Hershey, 1990; Chernyak, 1998; Li J and Stoica, 2009).

Suppression jamming and deceptive jamming are the main jamming strategies in actual electronic

---

countermeasures (ECMs) (Yu et al., 2019). Suppression jamming usually uses a high-power noise waveform to break down radar electronic protection measures. Its main purpose is to reduce the echo signal quality of the radar receiver, so the radar cannot perform target detection and tracking well. Deception jamming uses mainly the false target information to confuse the radar, so it does not confirm the distance or angle of the real target in the received echo information (Tang B et al., 2016). To improve target detection and tracking ability, radar systems need new anti-jamming strategies to deal with different types of jamming. In view of the gaming relationship between jamming and anti-jamming, decision makers on both sides need to change their own strategies to deal with the changing real-time battlefield information.

Recently, many studies have analyzed the communication network using game theory, which is mainly about the development of autonomous, anonymous, and flexible mobile networks. In fact, network devices can construct a low-complexity distributed algorithm that makes independent and reasonable strategic decisions concerning the cooperation and competition behaviors of network entities (Saad et al., 2009; Dahrouj and Yu, 2010; Moragrega et al., 2013). Game theory has also been applied to different aspects of radar research, including radar waveform design (Piezzo et al., 2013; Han and Nehorai, 2016; Panoui et al., 2016), radar countermeasures (Bachmann et al., 2011; Norouzi and Norouzi, 2012; Song et al., 2012; Deligiannis et al., 2016b; Wang and Zhang, 2019), target detection and tracking (Gogineni and Nehorai, 2012; Chavali and Nehorai, 2013; Tang L et al., 2013; Lan et al., 2015; Bogdanović et al., 2018; Niu et al., 2018), radar resource allocation (Sun et al., 2014; Chen et al., 2015; Deligiannis et al., 2016a, 2017; Shi et al., 2018; Liu et al., 2019; Yuan et al., 2019; Li ZJ et al., 2020; Shi et al., 2020a, 2021; Yi et al., 2020), and radar communication integration (Rihan and Huang, 2018; Shi et al., 2019a, 2019b, 2020b). Han and Nehorai (2016) considered the frequency-hopping waveform of collocated MIMO radar using game theory. The joint design of amplitude and frequency-hopping coding was used to meet the performance requirements of waveform design. Meanwhile, two joint algorithms were proposed and they converged to the $\epsilon$-approximate equilibrium. Similarly, a non-cooperative game the-

ory approach was considered in the coding design of radar networks (Piezzo et al., 2013). Three different non-cooperative game coding algorithms were proposed to minimize the sidelobe level, and these algorithms converged to the equilibrium solution of the game. Based on Piezzo et al. (2013), a novel game theory framework was constructed to study the waveform design of distributed MIMO radar in the presence of clutter. Moreover, the existence and uniqueness of Nash equilibrium (NE) were strictly proved using the large midpoint property (LMP) (Panoui et al., 2016). In the research on radar countermeasures, the interaction between the radars and jammers was evaluated in a typical and well-studied cluttered environment. A novel utility function with joint detection and false alarm probabilities was proposed. It was proved that the utility function satisfies the properties of supermodular games and the existence of pure strategy NE (Bachmann et al., 2011). Meanwhile, the mutual information criterion between the radars and jammers was taken as the utility function (Song et al., 2012). Unilateral, hierarchical, and symmetric games were studied, and the equilibrium solutions of power allocation were obtained. Additionally, strategic game theory analysis was applied to the scheduling between the radars and jammers during peace and war (Norouzi and Norouzi, 2012). In Tang L et al. (2013), the dynamic interactions between a bistatic radar network and an attacker were modeled as a repeated security game. Two learning algorithms were proposed, and were verified to converge to the set of correlated equilibria (Tang L et al., 2013). In Gogineni and Nehorai (2012), the target detection performance of polarization MIMO radar was investigated based on game theory. A game polarization target detection algorithm was proposed that has better performance than single vertical polarization or horizontal polarization (Gogineni and Nehorai, 2012). At the same time, with respect to target tracking, a game theoretic model for concurrent particle filter and data association was considered (Chavali and Nehorai, 2013). A particle filter technique for tracking maneuvering targets in the presence of clutter was used to build a regret-based learning algorithm to find this game's equilibrium. Aiming at the problems of power allocation between radars, a joint beamforming and power allocation technology was considered in the presence of multiple targets (Deligiannis et al.,

2016a). The relationship between radars using a strategic non-cooperative game (SNG) was studied. Furthermore, a power allocation learning algorithm was proposed, and it converged to the NE. Based on the cooperative relationship between radars, a power allocation strategy for a multistatic radar network in target tracking was analyzed using cooperative game theory (Sun et al., 2014; Chen et al., 2015). The performance of the proposed cooperative power allocation game (PAG) algorithm was better than those of random power allocation and uniform power allocation. In radar communication integration research, the Stackelberg game was used to study the PAG between radars and communication under spectrum coexistence (Shi et al., 2019b, 2020b). Furthermore, aiming at the uncertainty in radar communication integration, a robust Stackelberg game model was considered, in which the existence and uniqueness of the NE were strictly proved. Meanwhile, an iterative power allocation method was proposed, and it converged to the robust NE (Shi et al., 2019b).

Based on the above research, we study a game model between a multistatic MIMO radar network and multiple jammers with multiple targets. We do not consider the influence of clutter on the radars. For clarification, we can summarize the main contributions of this paper as follows:

1. Two kinds of supermodular game frameworks for joint power allocation and beamforming (JPAB) are established. One is a supermodular PAG framework with a fixed weight (FW) vector, while the other is a supermodular PAG framework based on an optimal beamforming weight vector.

2. Based on game theory analysis, the best response (BR) functions of the radars and jammers are obtained. Furthermore, the existence and uniqueness of NE are strictly proved.

3. The supermodular JPAB game algorithm is proposed, and it converges to the NE solution. In addition, the proposed algorithm can significantly suppress interference compared with other methods.

4. Numerical results are provided to verify the effectiveness and convergence of the algorithm.

Notations used in this paper are summarized as follows: $(\cdot)^{\mathrm{T}}$, $(\cdot)^*$, and $(\cdot)^{\mathrm{H}}$ represent the transpose, conjugate, and conjugate transpose operations, respectively. $\| \cdot \|_{\mathrm{F}}$ defines the Frobenius norm, $\| \cdot \|$ defines the Euclidean norm, and $| \cdot |$ represents the absolute value. $\boldsymbol{I}_L$ is an $L \times L$ identity matrix. $\mathbf{1}_L$ is

an all-one-vector whose length is $L$. $\boldsymbol{n}(t)$ is an independent and identically distributed Gaussian white noise at time $t$, with $\boldsymbol{n}(t) \sim \mathrm{CN}(\boldsymbol{0}, \sigma_n^2 \boldsymbol{I})$.

## 2  System model

A system model involving multistatic MIMO radars and multiple jammers with multiple targets is investigated, as shown in Fig. 1. There are $K$ separate multistatic radars, and every radar consists of $M_{\mathrm{t}}$ transmit antennas and $M_{\mathrm{r}}$ receive antennas. In particular, it is assumed that each radar is set to the same number of transmit and receive antennas; that is, $M = M_{\mathrm{t}} = M_{\mathrm{r}}$. The spacing between adjacent elements is a half wavelength. Multiple jammers emit jamming signals to decrease the target detection and tracking ability of the MIMO radars.
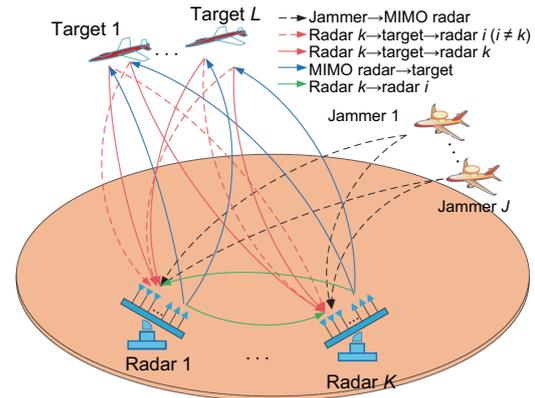


**Fig. 1  Multistatic MIMO radars and multiple jammers with multiple targets**

For multistatic radars, the precoding waveform sequence from the $k^{\mathrm{th}}$ radar to the $l^{\mathrm{th}}$ target is $s_{\mathrm{R}(kl)}(t)$, where $k = 1, 2, \cdots, K$, $l = 1, 2, \cdots, L$, and $t$ is the time index of the radar pulse. Then, the precoding waveform vector from the $k^{\mathrm{th}}$ radar can be expressed as $\boldsymbol{s}_{\mathrm{R}k}(t) = [s_{\mathrm{R}(k1)}(t), s_{\mathrm{R}(k2)}(t), \cdots, s_{\mathrm{R}(kL)}(t)]^{\mathrm{T}}$. In addition, the MIMO radar waveform vector meets the orthogonality conditions:

$$\int_{T_{\mathrm{R}}} \boldsymbol{s}_{\mathrm{R}k}(t) \boldsymbol{s}_{\mathrm{R}k}^{\mathrm{H}}(t) \mathrm{d}t = \boldsymbol{I}_L, \qquad (1)$$

where $T_{\mathrm{R}}$ denotes the waveform's pulse width.

The MIMO radar waveforms are uncorrelated for different targets. Based on acceptable time delays

$\tau_l$, the orthogonality satisfies

$$\int_{T_{\mathrm{R}}} s_{\mathrm{R}(kl)}(t - \tau_{kl}) s_{\mathrm{R}(kl')}^*(t - \tau_{kl'}) \mathrm{d}t = \begin{cases} 1, & l = l', \\ 0, & l \neq l'. \end{cases} \quad (2)$$

If a target echo is not completely orthogonal to the corresponding transmit waveform, the background noise will increase and the grating lobes will appear after the matched filtering. In this way, it will interfere with the radar's target detection ability.

The signal sequence transmitted by the $k^{\mathrm{th}}$ radar to the $l^{\mathrm{th}}$ target can be written as

$$\boldsymbol{x}_{\mathrm{R}(kl)}(t) = \boldsymbol{w}_{\mathrm{t}(kl)} s_{\mathrm{R}(kl)}(t), \quad (3)$$

where $\boldsymbol{w}_{\mathrm{t}(kl)}$ is the $M \times 1$ transmit beamforming weight vector from the $k^{\mathrm{th}}$ radar to the $l^{\mathrm{th}}$ target. Then, all the transmitted signals of the $k^{\mathrm{th}}$ radar can be obtained:

$$\boldsymbol{x}_{\mathrm{R}k}(t) = \sum_{l=1}^{L} \boldsymbol{w}_{\mathrm{t}(kl)} s_{\mathrm{R}(kl)}(t). \quad (4)$$

Thus, the reflected signals of the $k^{\mathrm{th}}$ radar from the angle $\theta_{kl}$ of the $l^{\mathrm{th}}$ target are

$$y_{\mathrm{R}(kl)}(t) = \beta_l \boldsymbol{w}_{\mathrm{t}(kl)}^{\mathrm{H}} \boldsymbol{a}(\theta_{kl}) s_{\mathrm{R}(kl)}(t), \quad (5)$$

where $\beta_l$ defines the $l^{\mathrm{th}}$ target reflection coefficient.

Then, the received signals of the $k^{\mathrm{th}}$ radar are

$$\tilde{\boldsymbol{y}}_{\mathrm{R}k}(t) = \sum_{i=1}^{K} \sum_{l=1}^{L} \boldsymbol{h}_{\mathrm{t}(kil)} s_{\mathrm{R}(il)}(t) + \sum_{j=1}^{J} \boldsymbol{c}_{\mathrm{t}(jk)} s_{\mathrm{J}(jk)}(t)$$
$$+ \sum_{i \neq k}^{K} \sum_{l=1}^{L} \boldsymbol{g}_{\mathrm{t}(kil)} s_{\mathrm{R}(il)}(t) + \boldsymbol{n}(t), \quad (6)$$

where $\boldsymbol{h}_{\mathrm{t}(kil)}$ is the channel vector for describing the channel response of the signal transmitted by the $i^{\mathrm{th}}$ radar, reflected by the $l^{\mathrm{th}}$ target, and received by the $k^{\mathrm{th}}$ radar, $\boldsymbol{g}_{\mathrm{t}(kil)}$ is the channel vector of the corresponding $l^{\mathrm{th}}$ target signal transmitted by the $i^{\mathrm{th}}$ radar and received by the $k^{\mathrm{th}}$ radar, and $\boldsymbol{c}_{\mathrm{t}(jk)}$ is the channel vector of the jamming signal received by the $k^{\mathrm{th}}$ radar and transmitted by the $j^{\mathrm{th}}$ jammer. Hence, the channel equations for transmitting/receiving sig-

nals are written as (Deligiannis et al., 2016a)

$$\boldsymbol{h}_{\mathrm{t}(kil)} = \boldsymbol{b}(\theta_{kl}) \boldsymbol{w}_{\mathrm{t}(il)}^{\mathrm{H}} \boldsymbol{a}(\theta_{il}) \beta_{kil}, \quad (7a)$$

$$\boldsymbol{h}_{\mathrm{r}(kil)} = \boldsymbol{a}(\theta_{il}) \boldsymbol{w}_{\mathrm{r}(kl)}^{\mathrm{H}} \boldsymbol{b}(\theta_{kl}) \beta_{kil}, \quad (7b)$$

$$\boldsymbol{g}_{\mathrm{t}(kil)} = \boldsymbol{b}(\theta_{\mathrm{rad}(ki)}) \boldsymbol{w}_{\mathrm{t}(il)}^{\mathrm{H}} \boldsymbol{a}(\theta_{\mathrm{rad}(ik)}), \quad (7c)$$

$$\boldsymbol{g}_{\mathrm{r}(kil)} = \boldsymbol{a}(\theta_{\mathrm{rad}(ki)}) \boldsymbol{w}_{\mathrm{r}(il)}^{\mathrm{H}} \boldsymbol{b}(\theta_{\mathrm{rad}(ik)}), \quad (7d)$$

$$\boldsymbol{c}_{\mathrm{t}(jk)} = \boldsymbol{b}(\theta_{kj}) \boldsymbol{w}_{\mathrm{t}(jk)}^{\mathrm{H}} \boldsymbol{a}(\theta_{jk}) \sqrt{p_{\mathrm{J}(jk)}}, \quad (7e)$$

$$\boldsymbol{c}_{\mathrm{r}(jk)} = \boldsymbol{a}(\theta_{jk}) \boldsymbol{w}_{\mathrm{r}(kj)}^{\mathrm{H}} \boldsymbol{b}(\theta_{kj}) \sqrt{p_{\mathrm{J}(jk)}}, \quad (7f)$$

where $\boldsymbol{w}_{\mathrm{r}(kl)}$ is the $M \times 1$ receive beamforming weight vector of the $k^{\mathrm{th}}$ radar to the $l^{\mathrm{th}}$ target, $\beta_{kil}$ is the radar cross section (RCS) reflection coefficient passing through the $l^{\mathrm{th}}$ target from the $i^{\mathrm{th}}$ radar to the $k^{\mathrm{th}}$ radar, $p_{\mathrm{J}(jk)}$ denotes the transmitted power of the $j^{\mathrm{th}}$ jammer after suppressed by the $k^{\mathrm{th}}$ radar, $\theta_{kl}$ represents the direction of arrival (DOA) from the $l^{\mathrm{th}}$ target to the $k^{\mathrm{th}}$ radar, $\theta_{\mathrm{rad}(ki)}$ is the direct direction angle from the $i^{\mathrm{th}}$ radar to the $k^{\mathrm{th}}$ radar, $\theta_{jk}$ is the DOA from the $j^{\mathrm{th}}$ jammer to the $k^{\mathrm{th}}$ radar, $\boldsymbol{a}(\theta)$ and $\boldsymbol{b}(\theta)$ are the transmitting and receiving steering vectors of the $k^{\mathrm{th}}$ radar respectively, which can be defined as

$$\boldsymbol{a}(\theta) = \left[ 1, \mathrm{e}^{\mathrm{j}d\frac{2\pi}{\lambda}\sin\theta}, \cdots, \mathrm{e}^{\mathrm{j}(M_{\mathrm{t}}-1)d\frac{2\pi}{\lambda}\sin\theta} \right]^{\mathrm{T}}, \quad (8a)$$

$$\boldsymbol{b}(\theta) = \left[ 1, \mathrm{e}^{\mathrm{j}d\frac{2\pi}{\lambda}\sin\theta}, \cdots, \mathrm{e}^{\mathrm{j}(M_{\mathrm{r}}-1)d\frac{2\pi}{\lambda}\sin\theta} \right]^{\mathrm{T}}, \quad (8b)$$

where $d$ is the array element spacing which is considered to be the same for all radars. Besides, $s_{\mathrm{J}(jk)}(t)$ indicates the jamming signal from the $j^{\mathrm{th}}$ jammer to the $k^{\mathrm{th}}$ radar in Eq. (6). Similarly, the jammer transmits the same signal as the radar does. Thus, the jamming waveform transmitted by the $j^{\mathrm{th}}$ jammer to the $k^{\mathrm{th}}$ radar is

$$s_{\mathrm{J}(jk)} = \sum_{l=1}^{L} w_{jkl} s_{\mathrm{R}(kl)}, \quad (9)$$

where $w_{jkl}$ denotes the weight coefficient of the jamming signal from the $j^{\mathrm{th}}$ jammer to the $k^{\mathrm{th}}$ radar corresponding to the $l^{\mathrm{th}}$ target. In this way, if the jamming signal is deceptive jamming, then it can be intensive false target jamming. If the jamming signal is suppression jamming, then it can be blanket jamming of white noise.

Although the receiver can obtain the desired target signal using matched filtering, there are jamming and cross-channel interference signals. Thus,

the matched filtering for the $l^{\text{th}}$ target echo is performed to obtain

$$
\begin{aligned}
\boldsymbol{z}_{\text{R}(kl)} = &\sum_{i=1}^{K}\sum_{n=1}^{L}\boldsymbol{h}_{\text{t}(kil)}\rho_{klin}(\tau_{ln}) + \sum_{j=1}^{J}\boldsymbol{c}_{\text{t}(jk)}\rho_{klj}(\tau_{lj}) \\
&+ \sum_{i\neq k}^{K}\sum_{n=1}^{L}\boldsymbol{g}_{\text{t}(kil)}\rho_{klin}(\tau_{ln}) + \boldsymbol{n},
\end{aligned}
\tag{10}
$$

where $\rho_{klin}(\tau_{ln})$ is the correlation factor between the $l^{\text{th}}$ target waveform transmitted by the $i^{\text{th}}$ radar and the corresponding $n^{\text{th}}$ target signal returning to the $k^{\text{th}}$ radar, and $\rho_{klj}(\tau_{lj})$ is the correlation factor between the jamming signal of the $j^{\text{th}}$ jammer and the signal transmitted from the $k^{\text{th}}$ radar to the $l^{\text{th}}$ target. Using beamforming, the desired output signal of the $k^{\text{th}}$ radar, which corresponds to the $l^{\text{th}}$ target, is

$$
Z_{\text{des}(kl)} = \boldsymbol{w}_{\text{r}(kl)}^{\text{H}}\boldsymbol{h}_{\text{t}(kkl)}.
\tag{11}
$$

The target detection and tracking abilities of radars will be affected by cross-channel and multi-jammer interference. In this way, the waveform corresponding to the $l^{\text{th}}$ target of the $k^{\text{th}}$ radar uses adaptive beamforming to suppress interference as follows:

$$
\begin{aligned}
Z_{\text{inter}(kl)} = &\sum_{i=1}^{K}\sum_{n\neq l}^{L}\boldsymbol{w}_{\text{r}(kl)}^{\text{H}}\boldsymbol{h}_{\text{t}(kil)}\rho_{klin}(\tau_{ln}) \\
&+ \sum_{j=1}^{J}\boldsymbol{w}_{\text{r}(kl)}^{\text{H}}\boldsymbol{c}_{\text{t}(jk)}\rho_{klj}(\tau_{lj}) \\
&+ \sum_{i\neq k}^{K}\sum_{n=1}^{L}\boldsymbol{w}_{\text{r}(kl)}^{\text{H}}\boldsymbol{g}_{\text{t}(kil)}\rho_{klin}(\tau_{ln}) + n,
\end{aligned}
\tag{12}
$$

where $n$ represents the Gaussian white noise.

$\gamma_{\text{R}(kl)}$ is the signal-to-interference-plus-noise ratio (SINR) of the $k^{\text{th}}$ radar corresponding to the $l^{\text{th}}$ target, written as

$$
\gamma_{\text{R}(kl)} = \frac{\left\|Z_{\text{des}(kl)}\right\|^{2}}{\left\|Z_{\text{inter}(kl)}\right\|^{2}}.
\tag{13}
$$

In this section, the system model is built. In the following section, the supermodular PAG is constructed, and the existence and uniqueness of the NE will be strictly proved.

# 3 Supermodular PAG with FW

## 3.1 Basic game formulation

A supermodular PAG framework is constructed in the presence of multiple targets between multistatic MIMO radars and multiple jammers. We study the suppression of jamming from the radar side, and clutter is not considered. The radars and jammers are the main players in the game, and their corresponding power can be regarded as the game strategies. The utility function is defined as a logarithmic function. The main purpose of MIMO radars is to maximize the utility function. Therefore, the game framework can be defined as

$$
\mathcal{G}_1 = \{\mathcal{P}_1, \mathcal{S}_1, \mathcal{U}_1\}.
\tag{14}
$$

(1) Player: $\mathcal{P}_1 = \mathcal{P}_{\text{R1}} \times \mathcal{P}_{\text{J1}}$, where $\mathcal{P}_{\text{R1}} = \{\text{Radar}_k | k = 1, 2, \cdots, K\}$ and $\mathcal{P}_{\text{J1}} = \{\text{Jammer}_j | j = 1, 2, \cdots, J\}$;

(2) Strategy: $\mathcal{S}_1 = \mathcal{S}_{\text{R1}} \times \mathcal{S}_{\text{J1}}$, where $\mathcal{S}_{\text{R1}} = \left\{p_{\text{R}(kl)} | \boldsymbol{p}_{\text{R}k} = \left[p_{\text{R}(k1)}, p_{\text{R}(k2)}, \cdots, p_{\text{R}(kL)}\right]^{\text{T}}\right\}$ and $\mathcal{S}_{\text{J1}} = \left\{p_{\text{J}(jk)} | \boldsymbol{p}_{\text{J}k} = \left[p_{\text{J}(1k)}, p_{\text{J}(2k)}, \cdots, p_{\text{J}(Jk)}\right]^{\text{T}}\right\}$;

(3) Utility function: $\mathcal{U}_1 = \left\{U_{\text{R}(klj)}\right\}$.

## 3.2 Power allocation optimization and NE analysis

In view of the interference effects of multiple jammers on multistatic MIMO radars, we need effective methods to suppress interference. In addition, a reasonable power allocation strategy is helpful in modifying radar's ability to suppress the jamming signal, which improves the radar's ability to detect and track targets. To obtain the radar power allocation strategy, we normalize the radar beamformer weight vectors as $\hat{\boldsymbol{w}}_{\text{t}(kl)} = \frac{\boldsymbol{w}_{\text{t}(kl)}}{\|\boldsymbol{w}_{\text{t}(kl)}\|}$ and $\hat{\boldsymbol{w}}_{\text{t}(jk)} = \frac{\boldsymbol{w}_{\text{t}(jk)}}{\|\boldsymbol{w}_{\text{t}(jk)}\|}$, and also denote $\hat{\sigma}^2 = \frac{\sigma^2}{\|\boldsymbol{w}_{\text{t}(kl)}\|^2}$. Therefore, the SINR can be rewritten as

$$
\gamma_{\text{R}(kl)} = \frac{\left|\boldsymbol{w}_{\text{r}(kl)}^{\text{H}}\hat{\boldsymbol{h}}_{\text{t}(kkl)}\right|^2 p_{\text{R}(kl)}}{\left|\boldsymbol{w}_{\text{r}(kl)}^{\text{H}}\hat{\boldsymbol{c}}_{\text{t}(jk)}\right|^2 p_{\text{J}(jk)} + \hat{\eta}_{\text{R}(kl)}}.
\tag{15}
$$

Furthermore, the total interference received by the $k^{\text{th}}$ radar corresponding to the $l^{\text{th}}$ target can be written as follows:

$$
I_{\text{R}(kl)} = \left|\boldsymbol{w}_{\text{r}(kl)}^{\text{H}}\hat{\boldsymbol{c}}_{\text{t}(jk)}\right|^2 p_{\text{J}(jk)} + \hat{\eta}_{\text{R}(kl)},
\tag{16}
$$

where $\hat{\boldsymbol{c}}_{\text{t}(jk)} = \boldsymbol{b}(\theta_{kj})\hat{\boldsymbol{w}}_{\text{t}(jk)}^{\text{H}}\boldsymbol{a}(\theta_{jk})$,

$$\hat{\eta}_{\text{R}(kl)} = \sum_{i\neq k}^{K}\sum_{n=1}^{L}\left|\boldsymbol{w}_{\text{r}(kl)}^{\text{H}}\hat{\boldsymbol{h}}_{\text{t}(kin)}\right|^{2}p_{\text{R}(in)} +$$

$$\sum_{n\neq l}^{L}\left|\boldsymbol{w}_{\text{r}(kl)}^{\text{H}}\hat{\boldsymbol{h}}_{\text{t}(kkn)}\right|^{2}p_{\text{R}(kn)} + \sum_{q\neq j}^{J}\left|\boldsymbol{w}_{\text{r}(kl)}^{\text{H}}\hat{\boldsymbol{c}}_{\text{t}(qk)}\right|^{2}p_{\text{J}(qk)}$$

$$+ \sum_{i\neq k}^{K}\sum_{n=1}^{L}\left|\boldsymbol{w}_{\text{r}(kl)}^{\text{H}}\hat{\boldsymbol{g}}_{\text{t}(kin)}\right|^{2}p_{\text{R}(in)} + \hat{\sigma}^{2}.$$

Then, from Eqs. (15) and (16), the following results can be obtained:

$$\gamma_{\text{R}(kl)} = \frac{\left|\boldsymbol{w}_{\text{r}(kl)}^{\text{H}}\hat{\boldsymbol{h}}_{\text{t}(kkl)}\right|^{2}p_{\text{R}(kl)}}{I_{\text{R}(kl)}}, \qquad (17)$$

$$\frac{\partial\gamma_{\text{R}(kl)}}{\partial p_{\text{R}(kl)}} = \frac{\left|\boldsymbol{w}_{\text{r}(kl)}^{\text{H}}\hat{\boldsymbol{h}}_{\text{t}(kkl)}\right|^{2}}{I_{\text{R}(kl)}} = \frac{\gamma_{\text{R}(kl)}}{p_{\text{R}(kl)}}, \qquad (18)$$

$$\frac{\partial\gamma_{\text{R}(kl)}}{\partial p_{\text{J}(jk)}} = -\frac{p_{\text{R}(kl)}\left|\boldsymbol{w}_{\text{r}(kl)}^{\text{H}}\hat{\boldsymbol{h}}_{\text{t}(kkl)}\right|^{2}\left|\boldsymbol{w}_{\text{r}(kl)}^{\text{H}}\hat{\boldsymbol{c}}_{\text{t}(jk)}\right|^{2}}{I_{\text{R}(kl)}^{2}}. \qquad (19)$$

For the supermodular PAG, we construct a logarithmic utility function as follows:

$$U_{\text{R}(klj)}(p_{\text{R}(kl)}, p_{\text{J}(jk)})$$
$$= \ln(\gamma_{\text{R}(kl)} - \gamma_{\text{R}(kl)}^{\min}) - \varepsilon_{kl}p_{\text{R}(kl)} + \sum_{q=1}^{J}\omega_{qk}p_{\text{J}(qk)}, \qquad (20)$$

where $\gamma_{\text{R}(kl)}^{\min}$ is the minimum SINR threshold, and $\varepsilon_{kl}$ and $\omega_{qk}$ are the linear price factor coefficients, which are positive numbers. Thus, the PAG optimization model is established by maximizing the utility function as follows:

$$\min_{\boldsymbol{p}_{\text{J}k}}\max_{\boldsymbol{p}_{\text{R}k}}\sum_{l=1}^{L}U_{\text{R}(klj)}(p_{\text{R}(kl)}, p_{\text{J}(jk)}) \qquad (21\text{a})$$

$$\text{s.t.} \quad \gamma_{\text{R}(kl)}^{\min} \leq \gamma_{\text{R}(kl)}, \quad \forall l, \qquad (21\text{b})$$

$$0 \leq p_{\text{R}(kl)} \leq p_{\text{R}(kl)}^{\max}, \quad \forall l, \qquad (21\text{c})$$

$$\boldsymbol{1}_{L}\boldsymbol{p}_{\text{R}k} \leq p_{\text{R}k}^{\text{Tot}}, \qquad (21\text{d})$$

$$0 \leq p_{\text{J}(jk)} \leq p_{\text{J}(jk)}^{\max}, \quad \forall j, \qquad (21\text{e})$$

$$\boldsymbol{1}_{J}\boldsymbol{p}_{\text{J}k} \leq p_{\text{J}k}^{\text{Tot}}, \qquad (21\text{f})$$

where $p_{\text{R}(kl)}^{\max}$ is the maximum transmitted power of the $k^{\text{th}}$ radar to the $l^{\text{th}}$ target, $p_{\text{J}(jk)}^{\max}$ is the maximum power of the $j^{\text{th}}$ jammer to the $k^{\text{th}}$ radar, $p_{\text{R}k}^{\text{Tot}}$ is the total transmitted power of the $k^{\text{th}}$ radar, and $p_{\text{J}k}^{\text{Tot}}$ is the total power from all the jammers to the $k^{\text{th}}$ radar.

To obtain the best power allocation strategies for the radars and jammers, the utility function is used to solve the BR functions of both sides. In this way, radars and jammers can allocate the power based on the BR strategies of the game. To maximize the radar's effectiveness, it is necessary to change its power allocation strategy to suppress the interference. The BR strategy of the $k^{\text{th}}$ radar to the $l^{\text{th}}$ target is as follows:

$$p_{\text{R}(kl)}^{*} = \arg\max_{p_{\text{R}(kl)}} U_{\text{R}(klj)}(p_{\text{R}(kl)}, p_{\text{J}(jk)}). \qquad (22)$$

Therefore, the closed-form BR function of the $k^{\text{th}}$ radar corresponding to the $l^{\text{th}}$ target can be obtained from Eq. (22) (the solution process is provided in the supplementary materials). We can obtain the result as follows:

$$p_{\text{R}(kl)}^{*} = \frac{\gamma_{\text{R}(kl)}^{\min}I_{\text{R}(kl)}}{\left|\boldsymbol{w}_{\text{r}(kl)}^{\text{H}}\hat{\boldsymbol{h}}_{\text{t}(kkl)}\right|^{2}} + \frac{1}{\varepsilon_{kl}}. \qquad (23)$$

To obtain the jammer's BR strategy, we use the utility function to obtain the BR function. Therefore, the BR strategy of the $j^{\text{th}}$ jammer corresponding to the $k^{\text{th}}$ radar is

$$p_{\text{J}(jk)}^{*} = \arg\min_{p_{\text{J}(jk)}} U_{\text{R}(klj)}(p_{\text{R}(kl)}, p_{\text{J}(jk)}). \qquad (24)$$

According to Eq. (24), we can obtain the quadratic equation of one unknown variable (the solution process is provided in the supplementary materials). We can obtain Eq. (25), given at the top of the next page.

Based on the quadratic root formula of one variable, we can obtain the BR closed-form solution of the jammers. To guarantee the nonnegativity of the power, we keep only the positive solution (26), given at the top of the next page.

According to Eqs. (16) and (26), we can obtain the BR closed-form solution from the $j^{\text{th}}$ jammer to the $k^{\text{th}}$ radar as

$$p_{\text{J}(jk)}^{*} = \frac{1}{\left|\boldsymbol{w}_{\text{r}(kl)}^{\text{H}}\hat{\boldsymbol{c}}_{\text{t}(jk)}\right|^{2}}\left(I_{\text{R}(kl)}^{*} - \hat{\eta}_{\text{R}(kl)}\right). \qquad (27)$$

Thus, the optimal power allocation strategies for the radars and jammers are obtained. According to the game theory, we can determine the NE solution of the game between the radars and jammers, as shown

$$I_{\mathrm{R}(kl)}^2 - \frac{p_{\mathrm{R}(kl)}\left|\boldsymbol{w}_{\mathrm{r}(kl)}^{\mathrm{H}}\hat{\boldsymbol{h}}_{\mathrm{t}(kkl)}\right|^2}{\gamma_{\mathrm{R}(kl)}^{\min}}I_{\mathrm{R}(kl)} + \frac{p_{\mathrm{R}(kl)}\left|\boldsymbol{w}_{\mathrm{r}(kl)}^{\mathrm{H}}\hat{\boldsymbol{h}}_{\mathrm{t}(kkl)}\right|^2\left|\hat{\boldsymbol{w}}_{\mathrm{r}(kl)}^{\mathrm{H}}\hat{\boldsymbol{c}}_{\mathrm{t}(jk)}\right|^2}{\omega_{jk}\gamma_{\mathrm{R}(kl)}^{\min}} = 0. \tag{25}$$

$$I_{\mathrm{R}(kl)}^* = \frac{p_{\mathrm{R}(kl)}\left|\boldsymbol{w}_{\mathrm{r}(kl)}^{\mathrm{H}}\hat{\boldsymbol{h}}_{\mathrm{t}(kkl)}\right|^2}{2\gamma_{\mathrm{R}(kl)}^{\min}} + \sqrt{\left(\frac{p_{\mathrm{R}(kl)}\left|\boldsymbol{w}_{\mathrm{r}(kl)}^{\mathrm{H}}\hat{\boldsymbol{h}}_{\mathrm{t}(kkl)}\right|^2}{2\gamma_{\mathrm{R}(kl)}^{\min}}\right)^2 - \frac{p_{\mathrm{R}(kl)}\left|\boldsymbol{w}_{\mathrm{r}(kl)}^{\mathrm{H}}\hat{\boldsymbol{h}}_{\mathrm{t}(kkl)}\right|^2\left|\boldsymbol{w}_{\mathrm{r}(kl)}^{\mathrm{H}}\hat{\boldsymbol{c}}_{\mathrm{t}(jk)}\right|^2}{\omega_{jk}\gamma_{\mathrm{R}(kl)}^{\min}}}. \tag{26}$$

in Fig. 2. The NE solution of the game means that no player can profit more by changing its unilateral strategy.
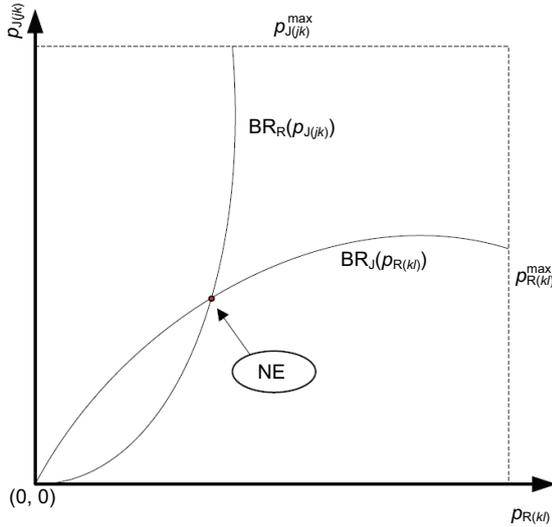


**Fig. 2   Nash equilibrium (NE) for the supermodular power allocation game**

To show that $\mathcal{G}_1$ is a supermodular game with a pure strategy NE solution, three properties of the supermodular game need to be satisfied: (1) The strategy set is a compact subset; (2) BR strategies of the utility function for all players are continuously differentiable; (3) The utility function satisfies the increasing difference in the relationship between the strategies of the players.

Obviously, the first two properties can be satisfied through the proposed game framework in this study. The third property can also be satisfied, and is equivalent to the second-order mixed partial derivative of the utility function of the strategies of both sides. The derivative result is greater than or equal to zero:

$$\frac{\partial U_{\mathrm{R}(klj)}^2(p_{\mathrm{R}(kl)},p_{\mathrm{J}(jk)})}{\partial p_{\mathrm{J}(jk)}\partial p_{\mathrm{R}(kl)}} \geq 0. \tag{28}$$

The proof of inequality (28) is provided in the supplementary materials.

**Lemma 1**   The utility function of the game has supermodularity, satisfying inequality (28).

Furthermore, the proposed game has supermodularity, and has pure strategy NE. Therefore, the existence of NE is satisfied. Next, the uniqueness of NE is proved using the standard function definition. The standard function satisfies the following three properties:

(1) Positivity. The function is strictly positive; that is, $F(x) > 0$.

(2) Monotonicity. If $x \geq x'$, then $F(x) \geq F(x')$.

(3) Scalability. For all $a > 1$, $aF(x) > F(ax)$.

The BR strategy of the $k^{\mathrm{th}}$ radar is derived as

$$\begin{aligned}&\mathrm{BR}_{\mathrm{R}}\left(p_{\mathrm{J}(jk)}\right)\\&= \frac{\gamma_{\mathrm{R}(kl)}^{\min}}{\left|\boldsymbol{w}_{\mathrm{r}(kl)}^{\mathrm{H}}\hat{\boldsymbol{h}}_{\mathrm{t}(kkl)}\right|^2}\left(\left|\boldsymbol{w}_{\mathrm{r}(kl)}^{\mathrm{H}}\hat{\boldsymbol{c}}_{\mathrm{t}(jk)}\right|^2 p_{\mathrm{J}(jk)} + \hat{\eta}_{\mathrm{R}(kl)}\right)\\&\quad + \frac{1}{\varepsilon_{kl}}.\end{aligned} \tag{29}$$

The proof of Eq. (29) is provided in the supplementary materials.

**Lemma 2**   BR function (29) satisfies the three properties of the standard function.

Therefore, the existence and uniqueness of NE are satisfied. After many game iterations, power allocation strategies of both sides converge to the NE. By replacing the variables in Eq. (29), we can obtain the iterative radar power allocation formula as follows:

$$p_{\mathrm{R}(kl)}^{(n+1)} = \left[\frac{\gamma_{\mathrm{R}(kl)}^{\min}}{\gamma_{\mathrm{R}(kl)}}p_{\mathrm{R}(kl)}^{(n)} + \frac{1}{\varepsilon_{kl}}\right]_0^{p_{\mathrm{R}(kl)}^{\max}}, \tag{30}$$

where $n$ is number of iterations and $[x]_a^b = \max[\min[x, b], a]$. In addition, according to Eq. (27), the corresponding iterative jammer power formula can be obtained as follows:

$$p_{\mathrm{J}(jk)}^{(n+1)} = \left[ \frac{1}{\left| \boldsymbol{w}_{\mathrm{r}(kl)}^{\mathrm{H}} \hat{\boldsymbol{c}}_{\mathrm{t}(jk)} \right|^2} \left( I_{\mathrm{R}(kl)}^{(n)} - \hat{\eta}_{\mathrm{R}(kl)}^{(n)} \right) \right]_0^{p_{\mathrm{J}(jk)}^{\max}}. \tag{31}$$

Based on the NE analysis of the above PAG, a reasonable power allocation strategy can help the radar maximize the utility values of the MIMO radars in the presence of multiple jammers. In this study, a supermodular PAG algorithm with an FW vector is proposed, as summarized in Algorithm 1.

---

**Algorithm 1** Supermodular PAG algorithm with FW

---

1: **Input:** Set the parameters and the initial power
2: **For** $l \leftarrow 1, L, k \leftarrow 1, K$
3:      Update radar power $p_{\mathrm{R}(kl)}$ using inequality (28)
4: **End For**
5: **For** $k \leftarrow 1, K, j \leftarrow 1, J$
6:      Update jammer power $p_{\mathrm{J}(jk)}^{(n)}$ using Eq. (29)
7: **End For**
8: **While** $\left| p_{\mathrm{R}(kl)}^{(n+1)} - p_{\mathrm{R}(kl)}^{(n)} \right| < \varepsilon$ **Stop**
9: **Output:** $p_{\mathrm{R}(kl)}$ and $p_{\mathrm{J}(jk)}$

---

In general terms, a supermodular PAG framework with FW is constructed. In this framework, we can obtain BR strategies of both sides of the game, and prove the existence and uniqueness of the NE. Based on the BR strategies, a supermodular PAG algorithm with FW is proposed to help the radar reduce the influence of jammers.

# 4 Supermodular game of JPAB

## 4.1 Basic game formulation

In this subsection, adaptive beamforming is used to suppress interference. Therefore, a supermodular PAG framework of JPAB is constructed, and the corresponding supermodular JPAB game algorithm is proposed to help the radar reduce the influence of jammers. The framework can be expressed as

$$\mathcal{G}_2 = \{\mathcal{P}_2, \mathcal{S}_2, \mathcal{U}_2\}. \tag{32}$$

(1) Player: $\mathcal{P}_{\mathrm{R}2} = \{\mathrm{Radar}_k | k = 1, 2, \cdots, K\}$ and $\mathcal{P}_{\mathrm{J}2} = \{\mathrm{Jammer}_j | j = 1, 2, \cdots, J\}$;

(2) Strategy: $\mathcal{S}_2 = \mathcal{S}_{\mathrm{R}2} \times \mathcal{S}_{\mathrm{J}2}$, where $\mathcal{S}_{\mathrm{R}2} = \left\{ \left( p_{\mathrm{R}(kl)}, \boldsymbol{w}_{\mathrm{t}(k1)} \right) | \boldsymbol{p}_{\mathrm{R}k} = \left[ p_{\mathrm{R}(k1)}, p_{\mathrm{R}(k2)}, \cdots, p_{\mathrm{R}(kL)} \right]^{\mathrm{T}}, \right.$
$\left. \boldsymbol{w}_{\mathrm{t}(k)} = \left[ \boldsymbol{w}_{\mathrm{t}(k1)}, \boldsymbol{w}_{\mathrm{t}(k2)}, \cdots, \boldsymbol{w}_{\mathrm{t}(kL)} \right]^{\mathrm{T}} \right\}$ and
$\mathcal{S}_{\mathrm{J}2} = \left\{ p_{\mathrm{J}(jk)} | \boldsymbol{p}_{\mathrm{J}k} = \left[ p_{\mathrm{J}(1k)}, p_{\mathrm{J}(2k)}, \cdots, p_{\mathrm{J}(Jk)} \right]^{\mathrm{T}} \right\}$;

(3) Utility function: $\mathcal{U}_2 = \left\{ U_{\mathrm{R}(klj)} \right\}$.

## 4.2 Beamforming optimization

To improve MIMO radar efficiency, we need to suppress different kinds of interference, including cross-channel interference, radar direct wave interference, and jammer interference. Adaptive beamforming can improve its own weight vector based on the external signal environment and internal processing system, and then effectively suppress the interference. There are classical optimal beamformer methods to solve adaptive weight vectors. These algorithms meet the radar system requirements based on optimal criteria, including the minimum mean square error (MMSE), minimum variance distortionless response (MVDR), and linearly constrained minimum variance (LCMV) (Frost, 1972; Souden et al., 2010; Yukawa et al., 2013). To determine the beamforming weight vector with game theory, the optimal radar receiving weight vector is obtained using the MMSE criterion in Deligiannis et al. (2016a). It can suppress cross-channel interference and strong clutter, such as a focal point. Although clutter is not considered, strong clutter can be effectively suppressed by the proposed algorithm. The MVDR and LCMV criteria are used to obtain the required beamforming weight vectors, and have better interference suppression effects. Next, the beamforming optimization model can be written as follows:

$$\min_{\boldsymbol{w}_{\mathrm{r}(kl)}} \quad \boldsymbol{w}_{\mathrm{r}(kl)}^{\mathrm{H}} \boldsymbol{R}_Z \boldsymbol{w}_{\mathrm{r}(kl)} \tag{33a}$$

$$\text{s.t.} \quad \boldsymbol{w}_{\mathrm{r}(kl)}^{\mathrm{H}} \boldsymbol{h}_{\mathrm{t}(kkl)} = 1, \tag{33b}$$

$$\boldsymbol{w}_{\mathrm{r}(kl)}^{\mathrm{H}} \boldsymbol{g}_{\mathrm{t}(kil)} = 0, \quad \forall i \neq k, \tag{33c}$$

$$\boldsymbol{w}_{\mathrm{r}(kl)}^{\mathrm{H}} \boldsymbol{c}_{\mathrm{t}(jk)} = 0, \quad \forall j, \tag{33d}$$

where $\boldsymbol{R}_Z = \sum_{i \neq 1}^{K} \sum_{n=1}^{L} p_{\mathrm{R}(in)} \hat{\boldsymbol{h}}_{\mathrm{t}(kin)} \hat{\boldsymbol{h}}_{\mathrm{t}(kin)}^{\mathrm{H}} + \sum_{n \neq l}^{L} p_{\mathrm{R}(kn)} \hat{\boldsymbol{h}}_{\mathrm{t}(kkn)} \hat{\boldsymbol{h}}_{\mathrm{t}(kkn)}^{\mathrm{H}} + \sigma_n^2 \boldsymbol{I}$. Let $\boldsymbol{G} = [\boldsymbol{h}_{\mathrm{t}(kkl)}, \underbrace{\boldsymbol{g}_{\mathrm{t}(k1l)}, \cdots, \boldsymbol{g}_{\mathrm{t}(kKl)}}_{K-1}, \underbrace{\boldsymbol{c}_{\mathrm{t}(1k)}, \cdots, \boldsymbol{c}_{\mathrm{t}(Jk)}}_{J}]$ and $\boldsymbol{F} = [1, \underbrace{0, \cdots, 0}_{K-1}, \underbrace{0, \ldots, 0}_{J}]$.

According to optimization model (33), we construct the optimization model constraint in the following matrix form:

$$\min_{\boldsymbol{w}_{\mathrm{r}(kl)}} \quad \boldsymbol{w}_{\mathrm{r}(kl)}^{\mathrm{H}} \boldsymbol{R}_Z \boldsymbol{w}_{\mathrm{r}(kl)} \tag{34a}$$

$$\text{s.t.} \quad \boldsymbol{w}_{\mathrm{r}(kl)}^{\mathrm{H}} \boldsymbol{G} = \boldsymbol{F}^{\mathrm{H}}. \tag{34b}$$

In this way, the Lagrange multiplier method is used to calculate the following results:

$$\begin{aligned} &L(\boldsymbol{w}_{\mathrm{r}(kl)}, \boldsymbol{\kappa}) \\ &= \frac{1}{2} \boldsymbol{w}_{\mathrm{r}(kl)}^{\mathrm{H}} \boldsymbol{R}_Z \boldsymbol{w}_{\mathrm{r}(kl)} + \left( \boldsymbol{w}_{\mathrm{r}(kl)}^{\mathrm{H}} \boldsymbol{G} - \boldsymbol{F}^{\mathrm{H}} \right) \boldsymbol{\kappa}, \end{aligned} \tag{35}$$

where $\boldsymbol{\kappa}$ is the Lagrangian multiplier vector. The gradient of Lagrangian function (35) can be obtained as

$$\nabla_{\boldsymbol{w}_{\mathrm{r}(kl)}} L(\hat{\boldsymbol{w}}_{\mathrm{r}(kl)}, \boldsymbol{\kappa}) = \boldsymbol{R}_Z \boldsymbol{w}_{\mathrm{r}(kl)} + \boldsymbol{G}\boldsymbol{\kappa} = \boldsymbol{0}. \tag{36}$$

Furthermore, the optimal receiving weight vector is obtained by solving Eq. (36) as

$$\boldsymbol{w}_{\mathrm{r}(kl)}^* = -\boldsymbol{R}_Z^{-1} \boldsymbol{G}\boldsymbol{\kappa}, \tag{37}$$

where $\boldsymbol{R}_Z$ exists and it is a positive definite matrix. The optimal receiving weight vector is substituted into the constraint of optimization model (34), and has the following result:

$$\boldsymbol{\kappa} = -\left( \boldsymbol{G}^{\mathrm{H}} \boldsymbol{R}_Z^{-1} \boldsymbol{G} \right)^{-1} \boldsymbol{F}. \tag{38}$$

Due to the existence of $\boldsymbol{G}^{\mathrm{H}} \boldsymbol{R}_Z^{-1} \boldsymbol{G}$, the positive definiteness of $\boldsymbol{R}_Z$, and the full rank of $\boldsymbol{G}$ (Frost, 1972), the optimal received beamforming weight is obtained from Eqs. (37) and (38):

$$\boldsymbol{w}_{\mathrm{r}(kl)}^* = \boldsymbol{R}_Z^{-1} \boldsymbol{G} \left( \boldsymbol{G}^{\mathrm{H}} \boldsymbol{R}_Z^{-1} \boldsymbol{G} \right)^{-1} \boldsymbol{F}. \tag{39}$$

In addition, the MVDR beamformer weight vector can be obtained by deforming the LCMV. According to Dahrouj and Yu (2010) and Deligiannis et al. (2016a), there is a scale coefficient relationship between the transmitting beamforming weight vector and the receiving beamforming weight vector:

$$\boldsymbol{w}_{\mathrm{t}(kl)} = \sqrt{\delta_{kl}} \boldsymbol{w}_{\mathrm{r}(kl)}, \tag{40}$$

where $\delta_{kl}$ is a scalar factor. This is calculated using the optimal equality form of SINR inequality constraint (21a). Therefore, substituting Eq. (40) into the SINR equality form in model (21), we have

$$\frac{1}{\gamma_{\mathrm{R}(kl)}^{\min}} \left| \boldsymbol{w}_{\mathrm{r}(kl)}^{\mathrm{H}} \hat{\boldsymbol{h}}_{\mathrm{r}(kkl)} \right|^2 \delta_{kl} - \sum_{n \neq l}^{L} \left| \boldsymbol{w}_{\mathrm{r}(kl)}^{\mathrm{H}} \hat{\boldsymbol{h}}_{\mathrm{r}(kkn)} \right|^2 \delta_{kn}$$

$$= \phi_{\mathrm{R}(kl)}, \tag{41}$$

where $\phi_{\mathrm{R}(kl)} = \sum_{i \neq k}^{K} \sum_{n=1}^{L} \left| \boldsymbol{w}_{\mathrm{r}(kl)}^{\mathrm{H}} \hat{\boldsymbol{h}}_{\mathrm{t}(kin)} \right|^2 p_{\mathrm{R}(in)} + \hat{\sigma}^2 +$ $\sum_{q=1}^{J} \left| \boldsymbol{w}_{\mathrm{r}(kl)}^{\mathrm{H}} \hat{\boldsymbol{c}}_{\mathrm{t}(qk)} \right|^2 p_{\mathrm{J}(qk)} + \sum_{i \neq k}^{K} \sum_{n=1}^{L} \left| \boldsymbol{w}_{\mathrm{r}(kl)}^{\mathrm{H}} \hat{\boldsymbol{g}}_{\mathrm{t}(kin)} \right|^2.$

Eq. (41) can be written as the following matrix form:

$$\boldsymbol{\Psi}_k \boldsymbol{\delta}_k = \boldsymbol{\phi}_k, \tag{42}$$

where $\boldsymbol{\delta}_k = [\delta_{k1}, \delta_{k2}, \cdots, \delta_{kL}]^{\mathrm{T}}$, and $\boldsymbol{\Psi}_k \in \mathbb{R}^{L \times L}$ and its corresponding elements can be expressed as $[\boldsymbol{\Psi}_k]_{ll} = \frac{1}{\gamma_{\mathrm{R}(kl)}^{\min}} \left| \boldsymbol{w}_{\mathrm{r}(kl)}^{\mathrm{H}} \boldsymbol{h}_{\mathrm{r}(kkl)} \right|^2$, $[\boldsymbol{\Psi}_k]_{lj} = -\left| \boldsymbol{w}_{\mathrm{r}(kl)}^{\mathrm{H}} \boldsymbol{h}_{\mathrm{r}(kkj)} \right|^2$, for $j \neq l$.

Therefore, an iterative supermodular JPAB game algorithm is proposed. The algorithm is summarized in Algorithm 2.

Finally, a supermodular JPAB game framework is constructed. The multistatic MIMO radar transmitting and receiving weight vectors are obtained, and the corresponding supermodular JPAB game algorithm is proposed.

---

**Algorithm 2** Supermodular JPAB game algorithm

---

1: **Input:** Set the parameters and the initial power
2: **For** $l \leftarrow 1, L, k \leftarrow 1, K$
3:     Update radar power $p_{\mathrm{R}(kl)}$ by inequality (28)
4:     Update receiving beamformer weight vector $\boldsymbol{w}_{\mathrm{r}(kl)}$ using Eq. (37)
5:     Update transmitting beamformer weight vector $\boldsymbol{w}_{\mathrm{t}(kl)}$ using Eq. (40)
6: **End For**
7: **For** $k \leftarrow 1, K, j \leftarrow 1, J$
8:     Update jammer power $p_{\mathrm{J}(jk)}^{(n)}$ using Eq. (29)
9: **End For**
10: **While** $\left| p_{\mathrm{R}(kl)}^{(n+1)} - p_{\mathrm{R}(kl)}^{(n)} \right| < \varepsilon$ **Stop**
11: **Output:** $p_{\mathrm{R}(kl)}$, $\boldsymbol{w}_{\mathrm{t}(kl)}$, $\boldsymbol{w}_{\mathrm{r}(kl)}$, and $p_{\mathrm{J}(jk)}$

---

## 5 Numerical results

In this section, numerical results are presented to verify the convergence and effectiveness of the proposed algorithms. It is assumed that each radar has the same number of transmit and receive array antennas, and that the distance between adjacent array elements is a half wavelength. The multistatic MIMO radars are on the same side, while the targets and jammers are on the opposite side. When multiple targets appear in the radar coverage area, the MIMO radars will accurately detect and track these targets. Then, the MIMO radars will guide the missile to strike and destroy the targets. However, to

decrease the radar's detection and tracking ability, the targets need to have super stealth and maneuverability and obtain jamming support from the same jammers. Therefore, the radars and jammers need to establish their own reasonable power allocation strategies in the game and gain the maximum profit.

Our model includes a bistatic MIMO radar network, two jammers, and two targets. On the radar system side, each radar consists of 24 transmit/receive antennas. The jammers use noise blanket jamming to interfere with radar operations. Therefore, the algorithms' parameters are set as follows: The DOAs of the targets' arrival at the radars are $\theta_{11} = 6°$, $\theta_{12} = 15°$, $\theta_{21} = 8°$, and $\theta_{22} = 32°$. The DOAs between the radars are $\theta_{\mathrm{rad}(12)} = 60°$ and $\theta_{\mathrm{rad}(21)} = -50°$. The DOAs of the jammers' arrival at the radars are $\theta_{11} = -60°$, $\theta_{12} = -40°$, $\theta_{21} = -20°$, and $\theta_{22} = 13°$. The minimum SINR thresholds are $\gamma_{11}^{\mathrm{min}} = 13$ dB, $\gamma_{12}^{\mathrm{min}} = 14$ dB, $\gamma_{21}^{\mathrm{min}} = 10$ dB, and $\gamma_{22}^{\mathrm{min}} = 12$ dB. The scattering amplitude coefficient of both targets is set to 1. The maximum power of each radar is 10. The maximum power of each jammer is set to 10. The tolerance of iteration difference is $10^{-8}$ or the termination step is 30. The price coefficients are set to $\varepsilon_{11} = 0.25$, $\varepsilon_{12} = 0.3$, $\varepsilon_{21} = 0.6$, $\varepsilon_{22} = 0.9$,

and $\omega_{11} = \omega_{12} = \omega_{21} = \omega_{22} = 0.8$. The correlation factor is 0.3. When two targets enter the radar power coverage, radars and targets become participants in the confrontation game. Meanwhile, the jammers interfere with the radars, which affects the normal radar operations. The decision makers control the radars to suppress the interference through reasonable power allocation strategies.

Fig. 3 shows the simulation results of the supermodular power allocation algorithm with FW. Fig. 3a shows the power allocation of multiple MIMO radars to different targets. After about 10 iterations, the algorithm converges to the NE. Fig. 3b shows the power allocation of two jammers to different radars. Fig. 3c shows various radar SINRs to the targets, which eventually converge to the preset minimum SINR thresholds. Fig. 3d shows the iterative convergence process of bistatic MIMO radar utility function values. According to the simulation results, the power allocation strategies of both sides converge to the NE of the game. In this way, the game players cannot unilaterally change their power allocation strategy to enhance their own advantage in the NE.

The influence of clutter on radars, however, is not considered in this study. For the supermodular
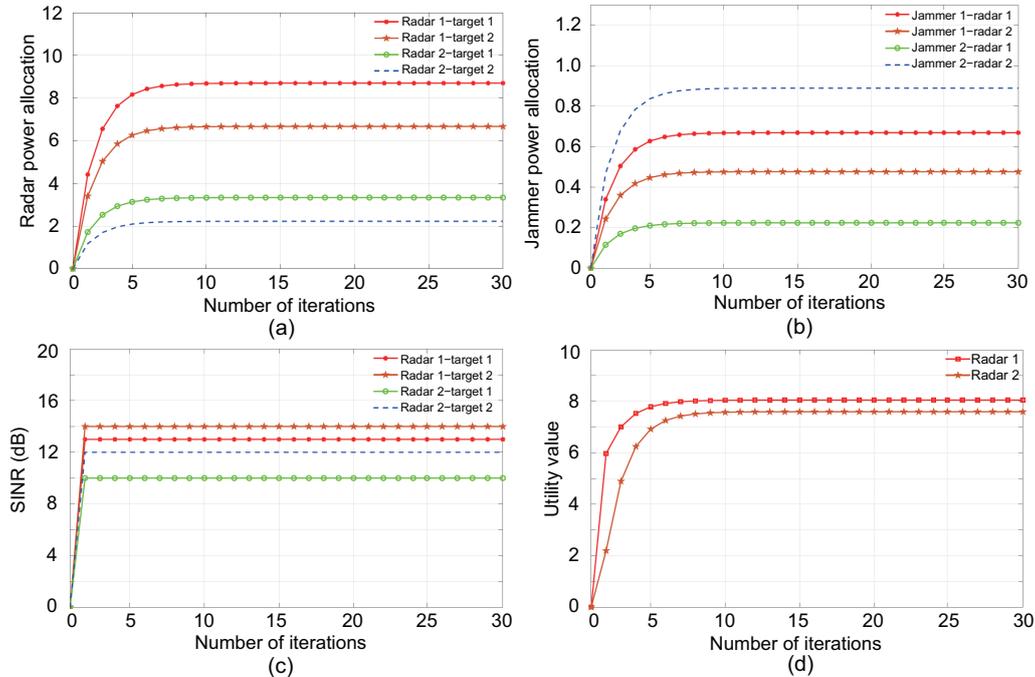


**Fig. 3  Simulation results of the supermodular PAG algorithm with FW: (a) power allocation convergence for MIMO radars; (b) power allocation convergence for jammers; (c) SINR convergence for MIMO radars; (d) utility value convergence for MIMO radars**

JPAB game algorithm, we construct MVDR and LCMV game algorithms. The simulation results are compared with those of the MMSE algorithm in Deligiannis et al. (2016a). Fig. 4 shows the receive beampatterns of different supermodular JPAB game algorithms. It can be seen from the figure that different targets are illuminated by multistatic MIMO radars. These three algorithms can suppress the cross-channel interference between radars. However, for jammer interference, the MMSE and MVDR game algorithms will show the angle deviation of interference suppression. The LCMV game algorithm can suppress the interference accurately. Fig. 5 shows a comparison of power allocation and utility function values between radars and jammers of all algorithms at the NE state. It shows that the MMSE, MVDR, and LCMV game algorithms cause multiple jammers to use more power than the FW algorithm under the same radar transmit power. Additionally, the utility values of the MMSE, MVDR, and LCMV game algorithms are larger than that of the FW algorithm. Finally, simulation results show that the LCMV game algorithm is better than the other algorithms.

# 6 Conclusions

Based on game theory analysis, we studied a game model of multistatic MIMO radars and multiple jammers in the presence of multiple targets. First, a supermodular game framework was established, in which radars and jammers were the main players that carried out power allocation strategies. The existence and uniqueness of NE of the game were strictly proved. Furthermore, a supermodular game algorithm with FW was proposed, and it converged to the NE. Then, a supermodular JPAB
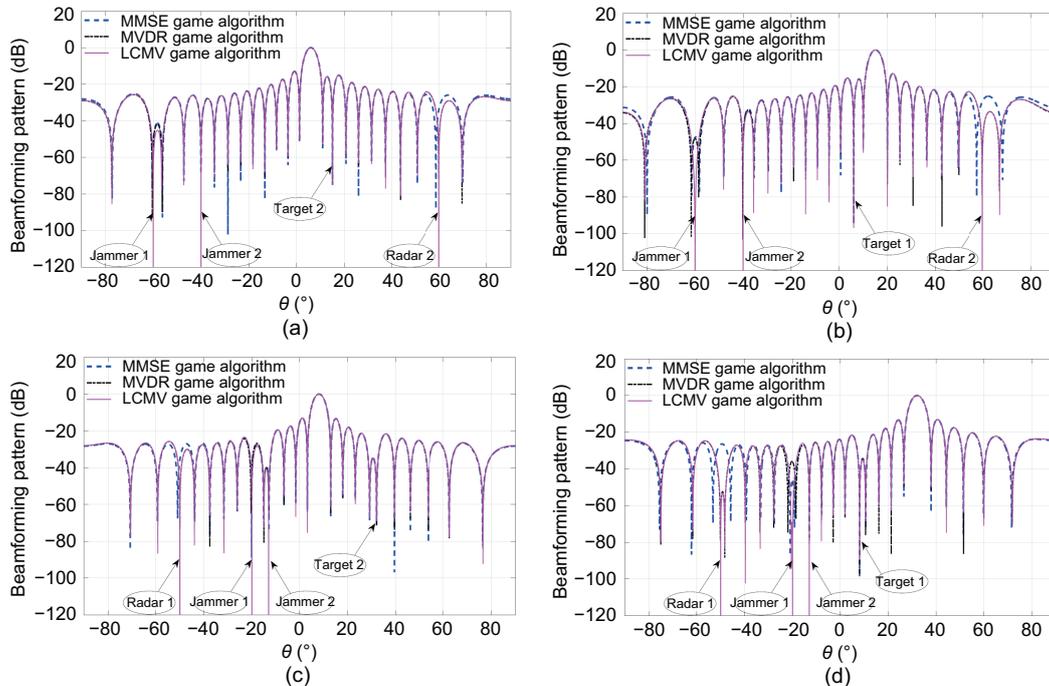


Fig. 5 **Performance comparison of different algorithms**



Fig. 4 **Receive beampatterns: (a) the main beam of radar 1 pointing to target 1; (b) the main beam of radar 1 pointing to target 2; (c) the main beam of radar 2 pointing to target 1; (d) the main beam of radar 2 pointing to target 2**
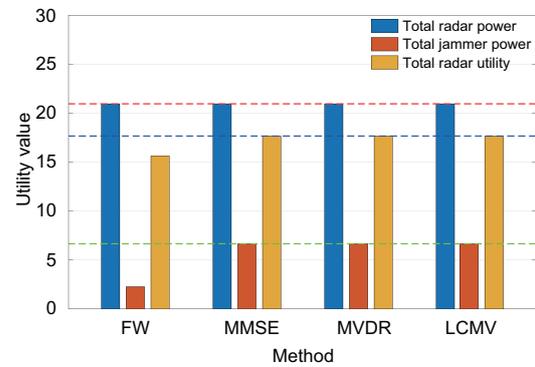
game framework was established to better suppress the interference of multiple jammers. Similarly, a supermodular JPAB game algorithm was proposed. To solve the received beamformer weight vector, we used MVDR and LCMV algorithms. According to the simulation results, the ability of the interference suppression and the effectiveness and convergence of the proposed algorithms were verified.

## Contributors

Bin HE and Hongtao SU designed the research. Bin HE processed the data and drafted the paper. Hongtao SU helped organize the paper. Bin HE and Hongtao SU revised and finalized the paper.

## Compliance with ethics guidelines

Bin HE and Hongtao SU declare that they have no conflict of interest.

## References

Bachmann DJ, Evans RJ, Moran B, 2011. Game theoretic analysis of adaptive radar jamming. *IEEE Trans Aerosp Electron Syst*, 47(2):1081-1100.
https://doi.org/10.1109/TAES.2011.5751244

Bogdanović N, Driessen H, Yarovoy AG, 2018. Target selection for tracking in multifunction radar networks: Nash and correlated equilibria. *IEEE Trans Aerosp Electron Syst*, 54(5):2448-2462.
https://doi.org/10.1109/TAES.2018.2819798

Chavali P, Nehorai A, 2013. Concurrent particle filtering and data association using game theory for tracking multiple maneuvering targets. *IEEE Trans Signal Process*, 61(20):4934-4948.
https://doi.org/10.1109/TSP.2013.2272923

Chen HW, Ta SY, Sun B, 2015. Cooperative game approach to power allocation for target tracking in distributed MIMO radar sensor networks. *IEEE Sens J*, 15(10):5423-5432.
https://doi.org/10.1109/JSEN.2015.2431261

Chernyak VS, 1998. Fundamentals of Multisite Radar Systems: Multistatic Radars and Multiradar Systems. Routledge, London, UK.

Dahrouj H, Yu W, 2010. Coordinated beamforming for the multicell multi-antenna wireless system. *IEEE Trans Wirel Commun*, 9(5):1748-1759.
https://doi.org/10.1109/TWC.2010.05.090936

Deligiannis A, Lambotharan S, Chambers JA, 2016a. Game theoretic analysis for MIMO radars with multiple targets. *IEEE Trans Aerosp Electron Syst*, 52(6):2760-2774. https://doi.org/10.1109/TAES.2016.150699

Deligiannis A, Rossetti G, Panoui A, et al., 2016b. Power allocation game between a radar network and multiple jammers. Proc IEEE Radar Conf, p.1-5.
https://doi.org/10.1109/RADAR.2016.7485077

Deligiannis A, Panoui A, Lambotharan S, et al., 2017. Game-theoretic power allocation and the Nash equilibrium analysis for a multistatic MIMO radar network. *IEEE*

Trans Signal Process*, 65(24):6397-6408.
https://doi.org/10.1109/TSP.2017.2755591

Frost III O, 1972. An algorithm for linearly constrained adaptive array processing. *Proc IEEE*, 60(8):926-935.
https://doi.org/10.1109/PROC.1972.8817

Gogineni S, Nehorai A, 2012. Game theoretic design for polarimetric MIMO radar target detection. *Signal Process*, 92(5):1281-1289.
https://doi.org/10.1016/j.sigpro.2011.11.024

Han KY, Nehorai A, 2016. Jointly optimal design for MIMO radar frequency-hopping waveforms using game theory. *IEEE Trans Aerosp Electron Syst*, 52(2):809-820.
https://doi.org/10.1109/TAES.2015.140408

Hershey JE, 1990. Counter-intuitive results cast in an electronic warfare framework. *IEEE Trans Aerosp Electron Syst*, 26(3):506-510.

Lan X, Li W, Wang XL, et al., 2015. MIMO radar and target Stackelberg game in the presence of clutter. *IEEE Sens J*, 15(12):6912-6920.
https://doi.org/10.1109/JSEN.2015.2466812

Li J, Stoica P, 2009. MIMO Radar Signal Processing. John Wiley & Sons, New York, USA.
https://doi.org/10.1002/9780470391488

Li ZJ, Xie JW, Zhang HW, et al., 2020. Adaptive sensor scheduling and resource allocation in netted collocated MIMO radar system for multi-target tracking. *IEEE Access*, 8:109976-109988.
https://doi.org/10.1109/ACCESS.2020.3001358

Liu XW, Zhang Q, Luo Y, et al., 2019. ISAR imaging task allocation for multi-target in radar network based on potential game. *IEEE Sens J*, 19(23):11192-11204.
https://doi.org/10.1109/JSEN.2019.2936423

Moragrega A, Closas P, Ibars C, 2013. Supermodular game for power control in TOA-based positioning. *IEEE Trans Signal Process*, 61(12):3246-3259.
https://doi.org/10.1109/TSP.2013.2259160

Niu C, Zhang YS, Guo JR, 2018. Pareto optimal layout of multistatic radar. *Signal Process*, 142:152-156.
https://doi.org/10.1016/j.sigpro.2017.07.017

Norouzi T, Norouzi Y, 2012. Scheduling the usage of radar and jammer during peace and war time. *IET Radar Sonar Navig*, 6(9):929-936.
https://doi.org/10.1049/iet-rsn.2012.0049

Panoui A, Lambotharan S, Chambers JA, 2016. Game theoretic distributed waveform design for multistatic radar networks. *IEEE Trans Aerosp Electron Syst*, 52(4):1855-1865.
https://doi.org/10.1109/TAES.2016.150378

Piezzo M, Aubry A, Buzzi S, et al., 2013. Non-cooperative code design in radar networks: a game-theoretic approach. *EURASIP J Adv Signal Process*, 2013(1):63.
https://doi.org/10.1186/1687-6180-2013-63

Rihan M, Huang L, 2018. Non-orthogonal multiple access based cooperative spectrum sharing between MIMO radar and MIMO communication systems. *Dig Signal Process*, 83:107-117.
https://doi.org/doi.org/10.1016/j.dsp.2018.07.014

Saad W, Han Z, Debbah M, et al., 2009. Coalitional game theory for communication networks. *IEEE Signal Process Mag*, 26(5):77-97.
https://doi.org/10.1109/MSP.2009.000000

Shi CG, Wang F, Sellathurai M, et al., 2018. Non-cooperative game-theoretic distributed power control technique for radar network based on low probability of intercept. *IET Signal Process*, 12(8):983-991. https://doi.org/10.1049/iet-spr.2017.0355

Shi CG, Wang F, Salous S, et al., 2019a. Distributed power allocation for spectral coexisting multistatic radar and communication systems based on Stackelberg game. Proc IEEE Int Conf on Acoustics, Speech and Signal Processing, p.4265-4269. https://doi.org/10.1109/ICASSP.2019.8683349

Shi CG, Qiu W, Wang F, et al., 2019b. Power control scheme for spectral coexisting multistatic radar and massive MIMO communication systems under uncertainties: a robust Stackelberg game model. *Dig Signal Process*, 94:146-155. https://doi.org/10.1016/j.dsp.2019.05.007

Shi CG, Ding LT, Wang F, et al., 2020a. Joint target assignment and resource optimization framework for multitarget tracking in phased array radar network. *IEEE Syst J*, 15(3):4379-4390. https://doi.org/10.1109/JSYST.2020.3025867

Shi CG, Ding LT, Wang F, et al., 2020b. Low probability of intercept-based collaborative power and bandwidth allocation strategy for multi-target tracking in distributed radar network system. *IEEE Sens J*, 20(12):6367-6377. https://doi.org/10.1109/JSEN.2020.2977328

Shi CG, Wang YJ, Wang F, et al., 2021. Joint optimization scheme for subcarrier selection and power allocation in multicarrier dual-function radar-communication system. *IEEE Syst J*, 15(1):947-958. https://doi.org/10.1109/JSYST.2020.2984637

Song XF, Willett P, Zhou SL, et al., 2012. The MIMO radar and jammer games. *IEEE Trans Signal Process*, 60(2):687-699. https://doi.org/10.1109/TSP.2011.2169251

Souden M, Benesty J, Affes S, 2010. A study of the LCMV and MVDR noise reduction filters. *IEEE Trans Signal Process*, 58(9):4925-4935. https://doi.org/10.1109/TSP.2010.2051803

Stephens JP, 1996. Advances in signal processing technology for electronic warfare. *IEEE Aerosp Electron Syst Mag*, 11(11):31-38. https://doi.org/10.1109/62.544024

Sun B, Chen HW, Wei XZ, et al., 2014. Power allocation for range-only localisation in distributed multiple-input multiple-output radar networks—a cooperative game approach. *IET Radar Sonar Navig*, 8(7):708-718. https://doi.org/10.1049/iet-rsn.2013.0260

Tang B, Li J, Zhang Y, et al., 2016. Design of MIMO radar waveform covariance matrix for clutter and jamming suppression based on space time adaptive processing. *Signal Process*, 121:60-69. https://doi.org/10.1016/j.sigpro.2015.10.033

Tang L, Gong XW, Wu JH, et al., 2013. Target detection in bistatic radar networks: node placement and repeated security game. *IEEE Trans Wirel Commun*, 12(3):1279-1289. https://doi.org/10.1109/TWC.2013.011713.120892

Wang LL, Zhang Y, 2019. MIMO radar and jammer power allocation game based on MMSE. Proc 20th Int Radar Symp, p.1-7. https://doi.org/10.23919/IRS.2019.8768191

Yi W, Yuan Y, Hoseinnezhad R, et al., 2020. Resource scheduling for distributed multi-target tracking in netted colocated MIMO radar systems. *IEEE Trans Signal Process*, 68:1602-1617. https://doi.org/10.1109/TSP.2020.2976587

Yu HL, Zhang J, Zhang LR, et al., 2019. Polarimetric multiple-radar architectures with distributed antennas for discriminating between radar targets and deception jamming. *Dig Signal Process*, 90:46-53. https://doi.org/10.1016/j.dsp.2019.03.012

Yuan Y, Yi W, Kirubarajan T, et al., 2019. Scaled accuracy based power allocation for multi-target tracking with colocated MIMO radars. *Signal Process*, 158:227-240. https://doi.org/10.1016/j.sigpro.2019.01.014

Yukawa M, Sung Y, Lee G, 2013. Dual-domain adaptive beamformer under linearly and quadratically constrained minimum variance. *IEEE Trans Signal Process*, 61(11):2874-2886. https://doi.org/10.1109/TSP.2013.2254481

# List of electronic supplementary materials

Proof S1  Proof of Eq. (23)
Proof S2  Proof of Eq. (25)
Proof S3  Proof of inequality (28)
Proof S4  Proof of Eq. (29)